

# Square patterns in Rayleigh-Bénard convection with rotation about a vertical axis

Kapil M. S. Bajaj, Jun Liu, Brian Naberhuis, and Guenter Ahlers

Department of Physics and Center for Nonlinear Science, University of California, Santa Barbara, California 93106, USA  
(November 8, 2018)

We present experimental results for Rayleigh-Bénard convection with rotation about a vertical axis at dimensionless rotation rates  $0 \leq \Omega \leq 250$  and  $\epsilon \equiv \Delta T / \Delta T_c - 1 \lesssim 0.2$ . Critical Rayleigh numbers and wavenumbers agree with predictions of linear stability analysis. For  $\Omega \gtrsim 70$  and small  $\epsilon$  the patterns are cellular with local four-fold coordination and differ from the theoretically expected Küppers-Lortz-unstable state. Stable as well as intermittent defect-free square lattices exist over certain parameter ranges. Over other ranges defects dynamically disrupt the lattice but cellular flow and local four-fold coordination is maintained.

PACS numbers: 47.54.+r, 47.20.Lz, 47.27.Te

The elucidation of spatio-temporal chaos (STC) remains one of the major tasks in the study of pattern formation in nonlinear dissipative systems. [1] The best opportunities for theoretical understanding of experimental observations of a chaotic state exist when the mean-square amplitude of STC evolves continuously (i.e. via a supercritical bifurcation) from a spatially-uniform ground state; for in that case it should be possible at least in principle to derive from the equations of motion of the system a systematic, simplified description in the form of Ginzburg-Landau equations. However, experimentally accessible supercritical bifurcations from the uniform state to STC are rare because most systems with supercritical primary bifurcations become variational as the threshold is approached from above and thus approach a time-independent state. Convection in a shallow horizontal layer of a fluid heated from below (Rayleigh-Bénard convection or RBC) and rotated about a vertical axis is one of the exceptions. Convection occurs when the temperature difference  $\Delta T$  exceeds a critical value  $\Delta T_c(\Omega)$  ( $\Omega$  is the rotation frequency) and leads to a velocity field  $\mathbf{v}$ . The Coriolis force  $\Omega \times \mathbf{v}$  renders the system non-variational even close to the convective threshold and thus permits the existence of STC at onset. Küppers and Lortz [2] (KL) predicted that a primary supercritical bifurcation leads to a state of unstable convection rolls provided  $\Omega > \Omega_{KL}$ . In this KL state, rolls of one orientation are unstable with respect to another set of rolls with an angular orientation relative to the first which is advanced in the direction of rotation by an angle  $\theta$ . [2,3,4] The new set, however, is equally unstable to yet another, and so forth. Several experiments confirmed the existence of the KL state at relatively large  $\epsilon \equiv \Delta T / \Delta T_c - 1$ . [5,6,7] Recent experiments [8,9,10] have shown its existence close to threshold for  $\Omega_{KL} \simeq 12 \lesssim \Omega \lesssim 20$  and have verified the supercritical nature of the bifurcation. The instability was observed to lead to a chaotically time dependent co-existence of domains with different roll orientations. Two examples [10] of this domain chaos are shown in Figs. 1a and b.

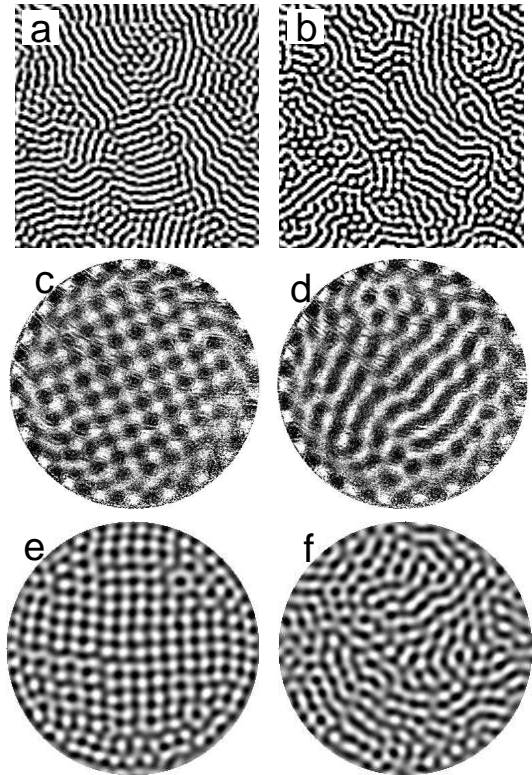


FIG. 1. Shadowgraph images of convection patterns viewed from above for  $\text{CO}_2$  (a and b, only parts of patterns are shown; adapted from Ref. [10]), water (c and d, the entire cell is shown), and Argon (e and f, 90% of the cell radius is shown) with  $(\sigma, \Omega, \Gamma)$  equal to  $(0.93, 19.8, 40)$ ,  $(5.4, 170, 4.8)$ , and  $(0.69, 181, 8.3)$  respectively. For small  $\Omega$  (a,b) the patterns have domains which are typical of the KL instability for all  $\epsilon$  near zero, as illustrated for  $\epsilon = 0.06$  (a) and  $0.18$  (b). At larger  $\Omega$ , square patterns occur close to onset [(c)  $\epsilon = 0.09$  and (e)  $\epsilon = 0.04$ ], but states similar to the KL domains are observed for  $\epsilon \gtrsim 0.1$  [ $\epsilon = 0.12$  in (d) and  $\epsilon = 0.13$  in (f)]. In c and d, the cells along the periphery are the wall mode.

Theoretically it is expected [2,3,4,11] that the nature of the bifurcation and of the nonlinear state above it should remain qualitatively unchanged as  $\Omega$  is increased above

the range explored previously by experiment. The measurements which we report here show that this is not the case. For  $\Omega \equiv 2\pi f d^2/\nu \gtrsim 70$  ( $f$  is the rotation frequency in Hz and  $\nu$  the kinematic viscosity) we find that the bifurcation does remain supercritical as predicted, but that the convection pattern above onset has no similarity to the expected KL state. Instead the pattern consists of cells which are usually arranged so as to have local four-fold coordination. Over significant parameter ranges the cells “crystallize” and form a square lattice. [12] Typical examples are shown in Figs. 1c and e. Depending on parameter values, the lattice can be stable, can be intermittently disrupted by defects which seem to be injected from the boundary, or can be continuously disorderd with many defects within it (maintaining, however, the cellular character with predominantly local four-fold coordination). At larger  $\epsilon$  ( $\epsilon \gtrsim 0.1$ ), we do observe patterns reminiscent of the KL state, as illustrated in Figs. 1d and f. The existence of the square state for  $\epsilon$ -values below those where the KL state is observed is contrary to theoretical prediction. This disagreement with theory occurs in a parameter range where the stability analysis was thought to be reliable, and thus presents a significant unresolved problem in the field of pattern formation. It also implies that the use of the KL state as a prototype for STC at onset is valid only at relatively small  $\Omega$ .

We used water and Argon in two different apparatus [13,14]. The Prandtl numbers  $\sigma \equiv \nu/\kappa$  ( $\kappa$  is the thermal diffusivity) were 5.4 and 0.69 respectively. The temperatures of the tops of the cells were regulated to  $\pm 1\text{mK}$  at  $30.07^\circ\text{C}$  (water) and at  $37.5^\circ\text{C}$  (Argon). Aspect ratios  $\Gamma \equiv r/d = 4.8$  and 8.3 ( $r$  is the radius and  $d$  the height of the fluid layer) were used for water ( $r = 38.1\text{ mm}$ ,  $d = 7.9\text{ mm}$ ) and Argon ( $r = 33.25\text{ mm}$ ,  $d = 4.0\text{ mm}$ ) respectively. The apparatus were rigidly mounted on rotating tables capable of rotation up to  $f = 1\text{ Hz}$ , covering the range  $0 \leq \Omega \leq 250$ . Shadowgraph assemblies were mounted ontop of the convection apparatus to obtain images in the rotating frame. For Argon, the pressure was controlled to  $\pm 2\text{mbar}$ . The experiments were carried out by raising the bottom-plate temperatures at fixed  $\Omega$ . Both heat-transport measurements and shadowgraph images were taken after waiting for at least a horizontal diffusion time  $\tau_h = \Gamma^2 d^2/\kappa$ . Onset was determined both from the heat transport and from amplitudes of the shadowgraph images.

The dimensionless control parameters are the Rayleigh number  $R \equiv \alpha g d^3 \Delta T / \kappa \nu$  and  $\Omega$ . Here  $\alpha$  is the isobaric thermal expansion coefficient,  $g$  the acceleration due to gravity, and  $\Delta T$  the temperature difference across the cell. The effect of centrifugal force given by the ratio of centrifugal-to-gravitational force  $F = 4\pi^2 f^2 r/g$  is less than 0.03 in most of the experiments and maximally 0.12 for a few runs. Since  $\Omega$  is scaled by  $\tau_\nu \equiv d^2/\nu$ , increasing the pressure  $P$  of Argon increased  $\Omega$  because it decreased  $\nu$ . We used this to vary  $\Omega$  by almost a factor of 4 at

fixed  $f$  (and thus  $F$ ). Increasing  $P$  changed  $\sigma$  only from 0.68 at 20 bar to 0.695 at 40 bar. It decreased the parameter  $Q$  [15] which describes the extent of departures from the Boussinesq approximation. For Argon  $Q$  ranged from 0.03 at 20 bar to 0.008 at 40 bar for the highest  $\Omega$  (largest  $\Delta T$ ). For water  $Q \simeq -0.02$  at large  $\Omega$ . Since  $Q$  was always small, we expect non-Boussinesq effects to be negligible.

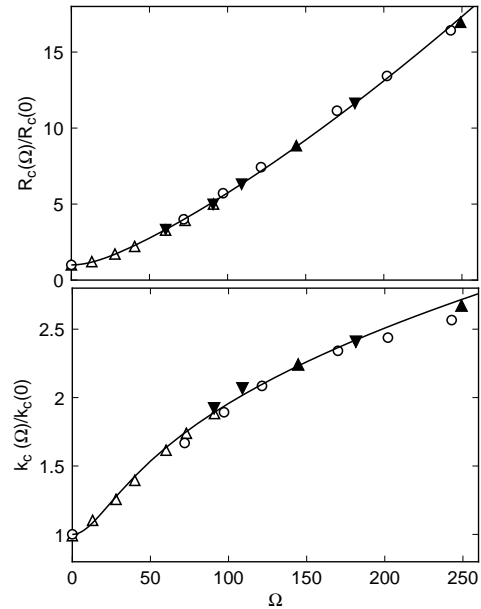


FIG. 2. The critical Rayleigh numbers  $R_c(\Omega)/R_c(0)$  (top) and wavenumbers  $k_c(\Omega)/k_c(0)$  (bottom) as a function of  $\Omega$  for water ( $\sigma = 5.4$ , open circles) and Argon at 20 bar ( $\sigma = 0.68$ , open triangles), 30 bar ( $\sigma = 0.69$  inverted solid triangles), and 40 bar ( $\sigma = 0.695$ , solid triangles). The results agree with the predictions for a laterally infinite system (solid lines) [16].

Figure 2 summarizes measurements of the critical Rayleigh numbers  $R_c(\Omega)$  and wavenumbers  $k_c(\Omega)$  for the onset of convection in the sample interiors (the “bulk mode”). The results agree with predictions based on linear stability analysis for a laterally infinite system. [16] These predictions are independent of  $\sigma$  and are given by the solid lines in Figs. 2. For  $\Omega \gtrsim 70$ , the bulk mode is preceded by a “wall mode” consisting of a wave traveling (in the rotating frame) in the direction opposite to  $\Omega$ . [17] The wall mode persists above  $R_c$ , and can be seen in Figs. 1c and d. The primary object of the present paper is the bulk mode.

Figure 3 shows shadowgraph images for  $\epsilon = 0.04$  for various  $\Omega$  in Argon. At small  $\Omega$  (Fig. 3a) the contrast of the image is poor because  $\Delta T$  and the wavenumber were small. Nonetheless one can see that almost the entire cell was occupied by a single domain of rolls. However, the time dependence of the pattern clearly revealed a dynamics characteristic of the KL state. [9,10] At somewhat larger  $\Omega$  (Fig. 3b) several KL domains exist simultane-

ously in the cell. These observations are consistent with previous work [9,10] using larger  $\Gamma$  and  $\Omega \lesssim 20$ . This situation changes when  $\Omega$  is increased beyond about 70, as illustrated by Figs. 3c and d. For  $\Omega = 73$ , the pattern is made up of cells rather than rolls. There are large domains where the pattern has square symmetry. Six domains of squares meet in the cell center and locally enforce a six-fold symmetry, maintaining however the cellular character of the flow. At larger  $\Omega = 145$  the pattern consists of a square lattice, with some domain walls and defects (right part of Fig. 3d) apparently provoked by the cell wall.

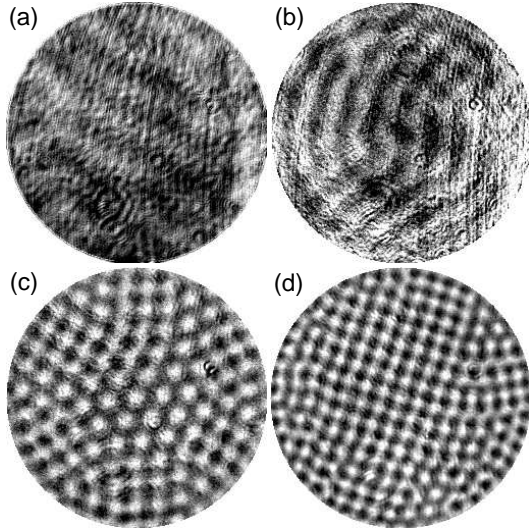


FIG. 3. Patterns for Argon and various  $\Omega$  at  $\epsilon \simeq 0.04$ .  $\Omega$  values are (a) 13, (b) 40 (c) 73 and (d) 145. Only 90% of the cell radius is shown. c and d are at the same physical rotation rate and at different pressures.

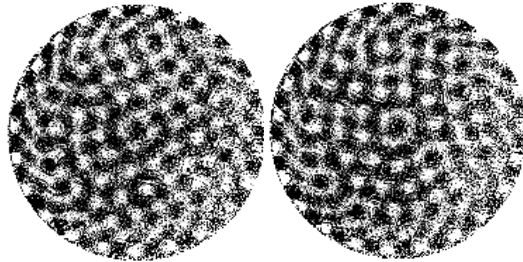


FIG. 4. Disordered cellular patterns for  $\sigma = 5.4$ ,  $\Omega = 170$ , and  $\epsilon = 0.052$ . The entire cell is shown. Along its periphery is the wall mode.

There are ranges of  $\Omega$ ,  $\epsilon$ , and  $\sigma$  over which the patterns near onset were dynamically disrupted by many defects, although cellular flow, often with local four-fold coordination, was maintained. Two examples for  $\sigma = 5.4$ ,  $\Omega = 170$ , and  $\epsilon = 0.052$  are shown in Fig. 4. In order to study the pattern dynamics in greater detail, we examined the time evolution of the structure function  $S(\mathbf{k})$

(the square of the modulus of the Fourier transform of the pattern). Two examples of  $S(\mathbf{k})$  are shown in Fig. 5.

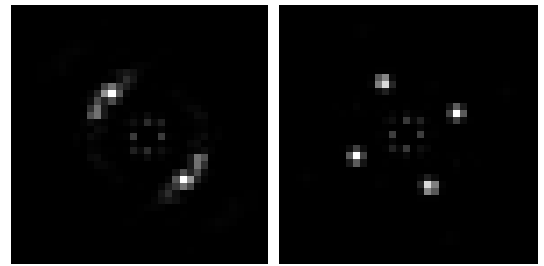


FIG. 5. Structure functions of images 1c (right) and 1d (left).

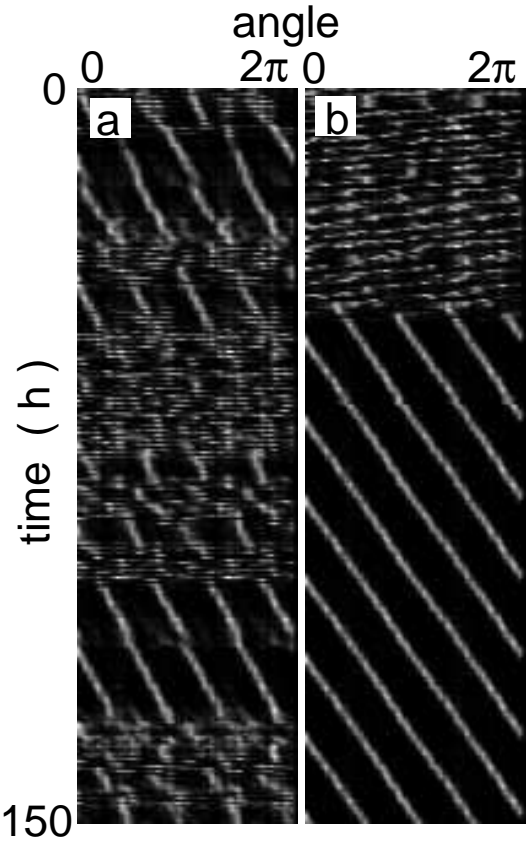


FIG. 6. Angle-time plot for the radial average of the structure function for  $\sigma = 5.4$  at  $\Omega = 170$  for (a)  $\epsilon = 0.072$  and (b)  $\epsilon = 0.091$ . (a) is a representative section of a long run. The system intermittently changes between a perfect square lattice and a disordered pattern with local four-fold coordination. For (b)  $\epsilon$  was stepped from 0.14 where the pattern was disordered (KL like) to 0.091 at time  $t = -3$  hours. After about  $16\tau_h$ , the system spontaneously chose the perfect-square pattern which then persisted for more than  $38\tau_h$ .

The left one is typical of the KL state, whereas the right one represents a square lattice. For  $\Omega = 170$  and  $\sigma = 5.4$ , the radial average  $S(\Theta)$  of  $S(\mathbf{k})$  is shown in Fig. 6 as a function of time. Figure 6a is a section of a long run at  $\epsilon = 0.072$ ; we believe it is representative of a static-

tically stationary process. Disordered regions alternate irregularly with well ordered square lattices. We believe the disorder is provoked by defects which are injected by interaction with the wall mode, but further work is required to examine the mechanism. Figure 6b is the result of an experiment where the system was kept in the KL regime at  $\epsilon = 0.14$  for a long time, and where at time  $t = -3$  hours  $\epsilon$  was reduced to 0.091. The system remained KL-like for nearly 44 hours (about 16 horizontal thermal diffusion times), and then *suddenly* crystallized into a square lattice which remained stable thereafter.

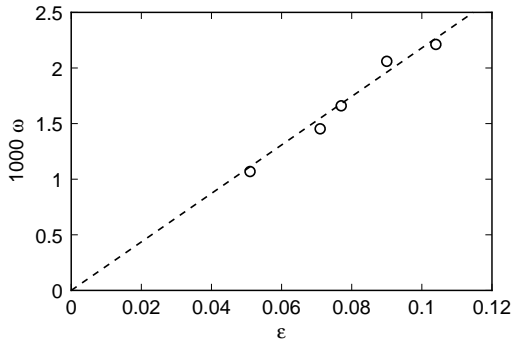


FIG. 7. The rotation rate  $\omega$  of the square lattice for  $\Omega = 170$  and  $\sigma = 5.4$ . Time is scaled by  $d^2/\nu$ .

It is interesting to note that the square lattice, whenever it exists, rotates at a rate  $\omega$  relative to the convection cell in the direction of the overall rotation  $\Omega$ , albeit extremely slowly. Results for  $\omega$  are given in Fig. 7. The measurements suggest that  $\omega$  vanishes as  $\epsilon$  goes to zero, as indicated by the dashed line. There is of course no theoretical prediction for  $\omega$ , since even the existence of the lattice is not understood. For comparison, under similar conditions the wall mode is travelling in the opposite direction at the much faster angular velocity of about  $-0.15\nu/d^2$ , nearly independent of  $\epsilon$ . We believe that the interaction between the fast-moving wall mode and the slow-moving bulk mode leads to the defect formation which tends to disrupt the square lattice for some parameter ranges.

Stable square patterns occur under other conditions in RBC. Convection of a pure fluid in a cell with insulating top and bottom plates [18] and binary-fluid convection with small Lewis numbers and a positive separation ratio [19] are two such systems. However, in those cases the critical wavenumber is reduced. Our critical wavenumbers agree with the linear stability analysis for rotating RBC of a pure fluid with perfectly conducting top and bottom boundaries. Our top and bottom boundaries have conductivities which are orders of magnitude larger than those of the fluids. Our Argon samples, even if they were contaminated with another component, would have Lewis numbers of order one [20] and thus would not produce a square pattern due to mixture effects. Clearly

impurities or poorly conducting boundaries cannot be invoked to explain our observations. Thus the occurrence of square patterns in rotating RBC at small  $\epsilon$  is unexplained, and we conclude that a real discrepancy exists between theory [2,3,4] and experiment.

We are grateful for stimulating discussions with F.H. Busse and W. Pesch. This work was supported by the U.S. Department of Energy Grant DE-FG03-87ER13738.

---

- [1] M. C. Cross and P. C. Hohenberg, *Rev. Mod. Phys.* **65**, 851 (1993).
- [2] G. Küppers and D. Lortz, *J. Fluid Mech.* **35**, 609 (1969).
- [3] G. Küppers, *Phys. Lett.* **32A** 7(1970).
- [4] R. Clever and F.H. Busse, *J. Fluid Mech.* **94**, 609 (1979).
- [5] H. E. Heikes, Ph. D. Dissertation, University of California, Los Angeles, unpublished, 1979.
- [6] F. H. Busse and K. E. Heikes, *Science* **208**, 173 (1980)
- [7] F. Zhong, R. E. Ecke and V. Steinberg, *Physica D* **51**, 596 (1991).
- [8] E. Bodenschatz, D.S. Cannell, R. Ecke, Y.C. Hu, K. Lerman, and G. Ahlers, *Physica D* **61**, 77 (1992).
- [9] Y.-C. Hu, R.E. Ecke, and G. Ahlers, *Phys. Rev. Lett.* **74**, 5040 (1995).
- [10] Y.-C. Hu, W. Pesch, G. Ahlers, and R.E. Ecke, *Phys. Rev. E*, unpublished.
- [11] F. Busse, private communication.
- [12] A square pattern near onset was observed indirectly by Heikes (Ref. [5]). However, that work did not have the optical resolution needed for direct observations. Instead, the system was equilibrated at small  $\epsilon$ , and then stepped to  $\epsilon = \mathcal{O}(1)$ . The rapidly growing amplitude then became observable, and suggested that the pattern at the previous steady state had been one of squares. To our knowledge these observations were never reported in the published literature.
- [13] G. Ahlers, D.S. Cannell, L.I. Berge, and S. Sakurai, *Phys. Rev. E* **49**, 545 (1994).
- [14] J.R. deBruyn, E. Bodenschatz, S. Morris, S. Trainoff, Y.-C. Hu, D.S. Cannell, and G. Ahlers, *Rev. Sci. Instrum.* **67**, 2043 (1996).
- [15] F. Busse, *J. Fluid Mech.* **30**, 625 (1967).
- [16] S. Chandrasekhar, *Proc. R. Soc. London* **A217**, 306 (1953); *Hydrodynamics and Hydromagnetic Stability*, Oxford University Press, London, 1961.
- [17] F. Zhong, R.E. Ecke, and V. Steinberg, *Phys. Rev. Lett.* **67**, 2473 (1991); *J. Fluid Mech.* **249**, 135 (1993); R. E. Ecke, F. Zhong and E. Knobloch, *Europhys. Lett.* **19**, 177 (1992); L. Ning and R.E. Ecke, *Phys. Rev. E* **47**, 3326 (1993); Y. Liu and R.E. Ecke, *Phys. Rev. Lett.* **78**, 4391 (1997).
- [18] F.H. Busse and N. Riahi, *J. Fluid Mech.* **96**, 243 (1980); M.R.E. Proctor, *J. Fluid Mech.* **113**, 469 (1981).
- [19] E. Moses and V. Steinberg, *Phys. Rev. A* **43**, 707 (1991); M.A. Dominguez-Lerma, G. Ahlers, and D.S. Cannell, *Phys. Rev. E* **52**, 6159 (1995).

[20] J. Liu and G. Ahlers, Phys. Rev. E **55**, 6950 (1997).